Salt-Triggered Intermembrane Exchange of Phospholipids and Hemifusion by Myelin Basic Protein†

Yolanda Cajal,*,‡ Joan M. Boggs,§ and Mahendra K. Jain*,‡

Department of Chemistry and Biochemistry, University of Delaware, Newark, Delaware 19716, and Department of Biochemistry, Research Institute, The Hospital for Sick Children, Toronto, Canada M5G 1X8

Received September 3, 1996; Revised Manuscript Received January 6, 1997⊗

ABSTRACT: Intervesicle phospholipid exchange through molecular contacts induced by the C1 molecular species of myelin basic protein (MBP) are characterized by using methods that amplify the effect of MBP−membrane interaction. The effect of salt concentration (KCl) on the vesicle−vesicle interaction of anionic sonicated covesicles of 30% 1-palmitoyl-2-oleoylglycero-*sn*-3-phosphocholine and 70% 1,2-dimyristoylglycero-*sn*-3-phosphomethanol (POPC/DMPM) by MBP is dissected by a combination of protocols into individual steps: aggregation of vesicles, apposition and contact formation, and hemifusion. Scattering and resonance energy transfer measurements reveal that, in the absence of KCl, MBP promotes rapid aggregation of the vesicles without lipid mixing. At >40 mM KCl, the extent of aggregation is larger and time-dependent. Fluorescence dequenching due to dilution of labeled phospholipids indicates that on a somewhat slower time scale, hemifusion of vesicles is triggered by salt, with mixing of the outer monolayer lipids but without flip-flop of phospholipids and without mixing or leakage of the aqueous contents. The exchange and hemifusion are seen with anionic vesicles; the effect of the structure of phospholipid, composition of vesicles, and the protein/lipid ratio is primarily on the kinetics of these and other competing processes. Thus, at 0.022 mol % of MBP and less than 100 mM KCl, it is possible to uncouple three sequential steps: (1) aggregation of vesicles by MBP; (2) apposition of bilayers and selective lipid exchange through vesicle−vesicle contacts established by MBP, i.e., anionic and zwitterionic phospholipids exchange, but cationic probes are excluded; and (3) hemifusion and lipid mixing of contacting monolayers of vesicles.

Myelin basic protein (MBP[1]), a major cytoplasmic component of the myelinated cells of the central nervous system, is believed to be responsible for the tight association of the cytoplasmic surfaces in compact myelin (Boggs et al., 1982). MBP binds preferentially to anionic bilayer surfaces (Gould & London, 1972; Boggs et al., 1977) and promotes aggregation and increase in permeability of vesicles (Epand et al. 1984; Papahadjopoulos et al., 1973). Since MBP has 24% hydrophobic and 19% positively charged residues at physiological pH, both electrostatic and hydrophobic interactions with the membrane are important (Boggs et al., 1980, 1982). Myelin is rich in anionic phospholipids, and binding of MBP may neutralize the surface charge on the cytoplasmic side. Resulting loss of electrostatic repulsive forces would facilitate MBP-mediated association of myelin layers by cross-linking the two apposed sides of the cytoplasmic membrane. It is not clear yet whether a monomer (Smith & McDonald, 1979) or a dimer of MBP (Smith, 1977) is involved in maintaining a close apposition between the cytoplasmic sides in myelin. In short, there is sufficient evidence for MBP−membrane interactions; however, neither the molecular details nor the functional significance of such interactions is known.

Changes in salt concentration could play a role in modulating MBP-mediated association of the intracellular surfaces in uncompacted regions of the myelin sheath such as the cytosol-containing paranodal loops, where the MBP concentration is lower than in compacted regions of myelin (Brunner et al., 1989; Omlin et al., 1982). Changes in cytosolic K^+ concentration may occur in the paranodal loops surrounding the nodes of Ranvier by uptake of K^+ released by the axon into the extracellular space around the node during the nerve action potential (Chiu, 1991). The ionic content of the paranodal loops is not known, but is likely to be similar to that found in oligodendrocyte: 60−74 mM for K^+ and 15 mM for Na^+ (Kettenman, 1987; Ballany & Kettenman, 1990).

In the present study, we have investigated the effects of salt concentration on the interaction of MBP with anionic lipid vesicles by adopting some of the remarkably sensitive methods developed by several research groups during the last decade for detection of bilayer apposition, lipid exchange, mixing, and fusion (Ellens et al., 1985; McIntyre & Sleight, 1991; Hoekstra et al., 1993; Düzgüneş & Wilshut, 1993; Hoekstra & Düzgüneş, 1993). Under suitable conditions, these protocols are well suited to amplify changes associated

† This work was supported by NIH (GM29703) and the Medical Research Council of Canada (MT 6506).

* To whom correspondence should be addressed.

‡ University of Delaware.

§ Hospital for Sick Children.

⊗ Abstract published in *Advance ACS Abstracts,* February 15, 1997.

[1] Abbreviations: ANTS, 1-aminonapthalene-3,6,8-trisulfonic acid; DMPG, 1,2-dimyristoylglycero-*sn*-3-phosphoglycerol; DMPM, 1,2-dimyristoylglycero-*sn*-3-phosphomethanol; DTPE-DNS, N-dansylated 1,2-ditetradecylglycero-*sn*-3-phosphoethanolamine; DPX, *N,N′-p*-xylenebis(pyridinium bromide); MBP, C1 species of bovine myelin basic protein; NBD-PE, *N*-(7-nitro-2−1,3-benzoxadiazol-4-yl)dioleoylphosphatidylethanolamine; POPC, 1-palmitoyl-2-oleoylglycero-*sn*-3-phosphocholine; POPG, 1-palmitoyl-2-oleoylglycero-*sn*-3-phosphoglycerol; PxB, polymyxin B; PyPC, 1-hexadecanoyl-2-(1-pyrenedecanoyl)-glycero-*sn*-3-phosphocholine; PyPM, 1-hexadecanoyl-2-(1-pyrenedecanoyl)glycero-*sn*-3-phosphomethanol; R18, octadecyl rhodamine; RET, resonance energy transfer; Rh-PE, *N*-(lissamine rhodamine B sulfonyl)-dioleoyl phosphatidylethanolamine; SUV, small unilamellar vesicles.

S0006-2960(96)02232-5 CCC: $14.00

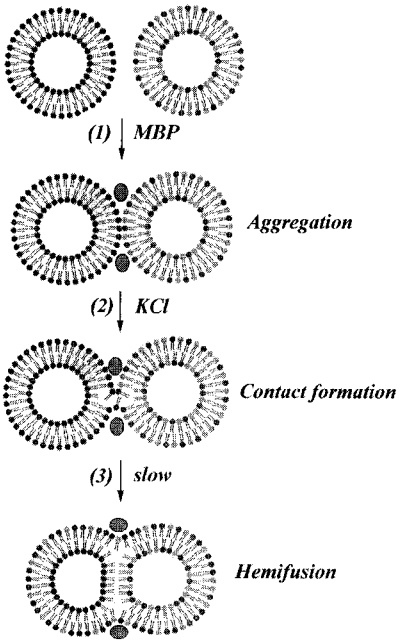

FIGURE 1: A proposed model for the interaction of MBP with anionic vesicles in the presence of salt. MBP aggregates anionic vesicles (step 1); after addition of salt, MBP establishes contacts that support selective exchange of phospholipids between the outer monolayers of the two apposed vesicles (step 2); after a lag period, complete mixing of the phospholipid in the outer monolayers takes place (hemifusion) (step 3).

with the formation of intervesicle contacts by a few molecules of MBP per vesicle and to demonstrate selective exchange of monoanionic phospholipids through the vesicle−vesicle contacts formed by MBP. In order to facilitate the presentation, a heuristic model for the interaction of MBP with small unilamellar vesicles (SUVs) of anionic phospholipids is shown in Figure 1. MBP-induced contacts are formed through a series of steps that depend on the salt concentration. MBP causes aggregation of vesicles in the absence of salt. KCl induces lipid exchange between the aggregated vesicles without fusion of the vesicles in contact. Under certain conditions it is possible to distinguish two sequential steps in the exchange of membrane components between the apposed vesicles: at lower KCl concentration there is a selective exchange of anionic and zwitterionic phospholipids, but not of cationic probes. At >70 mM KCl, a complete lipid mixing or hemifusion is seen, without leakage or mixing of the aqueous contents or merger of the distal monolayers.

MATERIALS AND METHODS

Reagents. Pyrene-labeled phospholipids (pyPM and pyPC), ANTS, DPX, and R18 were from Molecular Probes. POPC, POPG, DMPG, NBD-, and Rhodamine-phospholipids labeled at the amino group of phosphatidylethanolamines were from Avanti. Dithionite (sodium hydrosulfite) was from Mallinckrodt Chemical Works (St. Louis). DMPM (Jain et al., 1986) and DTPE-DNS were synthesized as described (Jain & Vaz, 1987). MBP was isolated from bovine brain white matter (Cheifetz & Moscarello, 1985) and fractionated into its charge isomers by ion-exchange chromatography at alkaline pH on CM52 (Chou et al., 1976; Cheifetz et al., 1984). The unmodified isomer C1 was isolated and showed primarily one band corresponding to the 18.5 KDa isomer of MBP by PAGE. Its concentration was calculated spectrophotometrically ($\epsilon = 11667\ M^{-1}\ cm^{-1}$). All manipulations were carried out in glass containers. All spectroscopic measurements were carried out with stirring in quartz cuvettes, in 10 mM Tris/1mM EGTA at pH 8.0 and 25 °C. Other specific conditions are given in the figure captions.

Preparation of Small Unilamellar Vesicles. Covesicles of DMPM containing 30% POPC alone or with the fluorescent probes NBD-PE, Rh-PE, DHPE-DNS, pyPM, or pyPC were prepared by evaporation of a mixture of the lipids in $CHCl_3/CH_3OH$ (2:1 v/v). The dried film was hydrated and then sonicated in a bath type sonicator (Lab Supplies, Hickesville, NY, Model G112SPIT) above the gel-fluid transition temperature until a clear dispersion was obtained (typically 2−4 min). R18 (6 mol %) was incorporated in the outer monolayers of preformed POPC/DMPM vesicles by adding an aliquot of vesicles to a tube with a film of R18 (formed from a stock solution in ethanol), and incubating for 60 min in the dark. For the ANTS/DPX fusion assay the vesicles contained 10 mM Tris pH 8.0 and either (i) 25 mM ANTS, (ii) 90 mM DPX, or (iii) 12.5 mM ANTS and 45 mM DPX. The vesicles were separated from unencapsulated material on Sephadex G-25 (Pharmacia), equilibrated with 10 mM Tris, pH 8.0. To calculate the lipid concentration after passage of the vesicles through the column, vesicles of the same composition but doped with 0.1% Rh-PE as a marker and without encapsulated material were filtered, and the amount of lipid recovered was calculated according to the Rh-PE fluorescence intensity taking the sample dilution into account. By this procedure, we calculate a 77 ± 10% lipid recovery and a dilution factor of 4 ± 0.4 (mean of 6 different samples). These vesicles were used within 10 h. Typically, the G-25 column could be reused 4−5 times after washing.

Asymmetrically Labeled POPC/DMPM/NBD-PE Vesicles. Vesicles of POPC/DMPM containing 0.6% NBD-PE incorporated in inner and outer monolayers were incubated in 0.2 mL of 10 mM Tris/1 mM EGTA buffer with 19 mM dithionite to selectively modify the NBD-PE groups present in the outer monolayer. After 5 min, the reaction mixture was diluted with more buffer to a final volume of 1.5 mL, with 54.4 μM lipid and 2.4 mM dithionite. At this point, all the outer membrane lipid has reacted with dithionite. Vesicles were used immediately after dilution.

Light Scattering. The change in turbidity was measured as the change in the 90° scattered intensity at 346 nm with 1 nm slit-widths on a SLM-Aminco AB-2 spectrofluorimeter. An aliquot of sonicated POPC/DMPM vesicles was added to the cuvette containing buffer, and then MBP was added from a stock solution, followed by KCl. The change in scattering was monitored continuously over 20 min with 6 s resolution. The effect of KCl alone on the turbidity of the vesicles was subtracted.

Fluorescence Assays for Lipid Mixing. Spectroscopic measurements were carried out on an AB-2 spectrofluorimeter (SLM-Aminco) with constant stirring. All spectral manipulations were carried out with the software provided with the instrument. Typically, the slit-widths were kept at 4 nm each and the sensitivity (PMT voltage) was set for the buffer blank to 1% for the Raman peak corresponding to the same excitation wavelength.

(i) Monitored as Change in Monomer Emission of pyPM or pyPC by Surface Dilution. The exchange of lipid between

vesicles on the addition of MBP (with or without KCl) was assessed by monitoring transfer of pyrene-labeled phospholipids from covesicles of pyPM/POPC (70:30) or pyPC/DMPM (70:30) to 125-fold excess of unlabeled phospholipid vesicles as acceptors. Fluorescence emission was monitored at 395 nm (with excitation at 346 nm) corresponding to the monomer emission. The relative change in fluorescence is given as $[(F - F_o)/(F_{max} - F_o)] \times 100$, where F is the fluorescence after the addition of KCl to the MBP-containing vesicles, F_o is the fluorescence in the absence of MBP, and F_{max} is the fluorescence after total mixing of lipids, measured by the addition of detergent (2.2 mM deoxycholate) under conditions where the excimer peak at 480 nm is negligible.

(ii) Monitored as Release of Self-Quenching. Lipid mixing induced by MBP was monitored by measuring the release of self-quenching of 6 mol % R-18 incorporated in the outer monolayer of POPC/DMPM vesicles or by monitoring release of quenching of 20% Rh-PE incorporated in both inner and outer layers of the covesicles. The labeled vesicles were mixed with unlabeled POPC/DMPM vesicles in 1:125 mol ratio, and the fluorescence increase at 577 nm (excitation 556 nm) upon the addition of MBP with or without KCl in the medium was recorded for 20 min. The relative change in the fluorescence, δF, is defined as $(F - F_o)/F_o$, where F_o and F are the intensities without and with MBP, respectively.

(iii) Vesicle Apposition and Lipid Mixing by Resonance Energy Transfer (RET). The vesicle mixture used for RET contained 0.6% of NBD-PE or Rh-PE codispersed with POPC/DMPM with excitation for NBD at 460 nm, the fluorescence emission from rhodamine at 592 nm has only a small contribution from NBD fluorescence. The change in fluorescence was calculated as $[F - F_o]/[F_{max} - F_o]$, with F_o and F corresponding to the fluorescence intensities before and after the addition of MBP and F_{max} as the fluorescence after total mixing of lipids, measured with covesicles containing 0.3 mol % of each of the probes at the same total bulk lipid concentration. This protocol was also used to monitor hemifusion-induced dilution of the probes in excess unlabeled vesicles (ratio 1:50). Asymmetrically labeled NBD-PE vesicles, where the NBD groups in the outer monolayer were chemically quenched by reaction with dithionite, were used to monitor mixing of phospholipids in the inner monolayers.

ANTS/DPX Fusion Assay for Leakage or Mixing of Aqueous Compartments. Dequenching of coencapsulated ANTS and DPX fluorescence resulting from dilution was measured to assess leakage of aqueous contents (Ellens et al., 1985). Excitation was set at 360 nm, and emission at 530 nm was recorded as a function of time. The scale was calibrated with the fluorescence of the 1:1 mixture of ANTS and DPX loaded vesicles taken as 100% leakage; the fluorescence of the same concentration of vesicles containing coencapsulated ANTS and DPX was taken as 0% leakage. The fluorescence of the lysed vesicles containing both ANTS and DPX (using 2.2 mM deoxycholate) is the same as the fluorescence of the mixture of vesicles with ANTS and vesicles with DPX (1:1 ratio). To determine if nonleaky fusion occurs, ANTS and DPX were encapsulated in separate populations of vesicles and mixed in a 1:1 ratio. Nonleaky fusion results in mixing of aqueous contents and a decrease in ANTS fluorescence due to quenching of ANTS by DPX.

Binding Isotherms. The binding of MBP to POPC/DMPM vesicles containing 2% of either NBD-PE or DTPE-DNS was determined as the increase in the intensity of the RET signal from Trp to the labeled phospholipid at 535 nm (excitation 285 nm). Vesicles in buffer with and without KCl were titrated with MBP from a stock solution 0.175 mM in water, and stoichiometry was determined directly from the plot of δF vs MBP/Lipid (mol:mol). Since the lipid concentration was low (21.8 μM), the contribution from light scattering was less than 3%.

Fluorescence Assay Using Dithionite to Determine the Accessibility of Phospholipids in POPC/DMPM Vesicles. Reaction of small sonicated vesicles containing NBD-PE with dithionite selectively eliminates the fluorescence signal derived from NBD present in the outer leaflet by a reduction reaction (McIntyre & Sleight, 1991; Hoekstra et al., 1993). An aliquot of POPC/DMPM covesicles doped with 0.6% NBD-PE, was added to 1.5 mL of 10 mM Tris/1mM EGTA buffer (pH 8.0) saturated with nitrogen, with constant stirring (lipid concentration 110 μM). When a stable baseline was achieved (usually less than 60 s after the addition), the reaction was started by adding dithionite from a stock solution to a final concentration of 20 mM. The time-dependent decrease in the fluorescence at 535 nm was recorded for 800 s (resolution 1 s). Excitation wavelength was set at 460 nm with both slit-widths at 4 nm. Stock solutions of freshly prepared 1.44 M dithionite in 0.5 M Na_2CO_3 (pH 11) buffer saturated with nitrogen gas, were stored at 0 °C and used within 1 h.

RESULTS

MBP Induces Apposition of POPC/DMPM Vesicles. Addition of MBP to a population of SUVs of POPC/DMPM results in a significant increase in light scattering as shown in Figure 2A. This effect of MBP has been reported for other anionic vesicles (Jo & Boggs, 1995; Epand et al., 1984; Lampe et al., 1983; Cheifetz & Moscarello, 1985; Walker & Rumby, 1985). The increase in scattering is seen at very low concentrations of MBP; the lowest point in this figure at 0.006 mol % corresponds to <1 MBP per vesicle. These results show that MBP induces an increase in the size of the particles, as indicated in the first step of Figure 1, and the underlying biophysical changes are characterized below.

Larger Particles Are Formed in the Presence of KCl. The effect of MBP on the aggregation of anionic vesicles of POPC/DMPM is accentuated by the presence of KCl. At 133 mM KCl the turbidity increase reaches a plateau at 0.022 mol % of MBP. A several-fold increase is seen in the presence of salt compared to the increase in scattering seen without salt (Figure 2A). These results show that MBP in the presence of KCl is more effective in inducing aggregation, which confirms the observations of Jo and Boggs (1995). Nevertheless, the overall process is more complex. For example, the time course of the change in scattering initiated by <100 mM KCl added to a mixture of POPC/DMPM and MBP (0.022 mol %) shows a biphasic change (Figure 2B). The rapid phase is completed in less than 10 s, and it is followed by a lag period where the scattering intensity does not change. At the end of the lag period there is a further time-dependent increase in turbidity. The lag period decreases with increasing salt concentration. At KCl concentrations above 100 mM, the lag period is <50 s, and the two phases were not adequately resolved by the methods at hand.

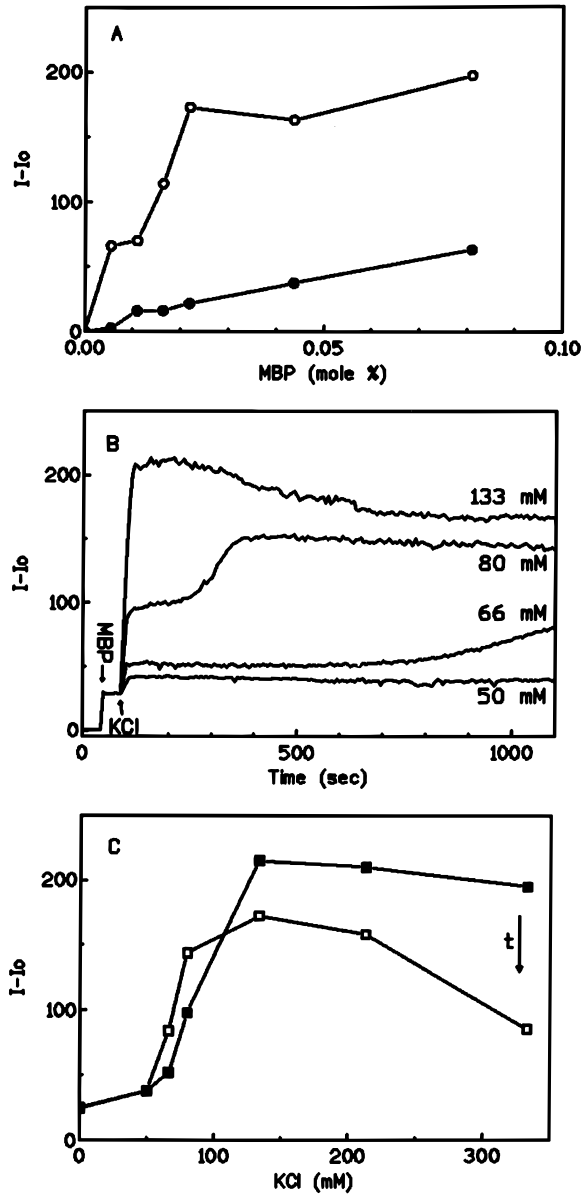

FIGURE 2: Changes in the intensity of 90° scattered light of POPC/DMPM vesicles (211 μM) caused by MBP. (Panel A) Increase in scattering as a function of MBP in the absence (●) or in the presence (○) of 132 mM KCl; MBP was added to the vesicles from a stock solution (17.45 μM), followed by KCl. (Panel B) Time-course of the change in scattering; MBP (0.047 μM) was added to POPC/DMPM vesicles, followed by KCl. (Panel C) Change in scattering immediately after KCl addition (■) and at 15 min (□). The direct effect of KCl on the scattering of protein-free vesicles was subtracted as the background; typically, this effect was <10% below 200 mM KCl, but significant at higher concentrations. The effect of MBP without salt is instantaneous and does not change with time for at least 60 min.

The change in scattering by 0.022 mol % MBP shows a complex dependence on KCl concentration (Figure 2C): If the overall scattering change is plotted, a modest increase is followed by a steep increase in scattering at low salt concentrations that reaches a maximum at 133 mM KCl. As shown in Figure 2C, at >80 mM KCl there is a time-dependent decrease in scattering 200 s after the initial mixing. Such a decrease in the scattered light intensity is probably due to formation of larger clusters due to charge shielding induced by higher concentrations of the salt (Walker & Rumby, 1985; Jo & Boggs, 1995).

Phospholipid Exchange by MBP Occurs Only in the Presence of Salt. We used some of the well-established assays to determine if the increase in 90° scattering from vesicles induced by MBP with or without KCl (Figure 2) is simply due to an aggregation or clustering of vesicles or if there are also functional changes such as exchange of phospholipids. The labeled phospholipid pyPM in covesicles with 30% POPC shows significant excimer fluorescence at 480 nm, with very little contribution from the monomer at 395 nm. Exchange with excess unlabeled covesicles of POPC/DMPM is not induced by MBP in the absence of salt (Figure 3A), because only an insignificant increase of monomer fluorescence occurs over a wide range of MBP concentrations. On the other hand, as shown in Figure 3A, in the presence of 133 mM KCl the increase in monomer signal due to lipid mixing is proportional to the MBP mole fraction. As shown in Figure 3, panels B and C, the extent of lipid mixing is time-dependent and also depends on the salt concentration. The time-course of lipid mixing shows a biphasic behavior depending on the salt concentration (Figure 3B). Below 133 mM KCl, the effect of MBP is characterized by an initial fast exchange of pyPM followed by a lag period and a second phase of lipid exchange which has a time-dependent component. At KCl concentrations above 133 mM, only the fast component is seen, and the extent at 15 min is higher. The extent of lipid mixing corresponding to the two time-dependent phases (Figure 3B) is shown in Figure 3C, where a plateau is reached at 200 mM KCl. Controls also showed that KCl has no effect on the exchange of pyPM in the absence of MBP.

To determine if MBP shows selectivity for the exchange of phospholipids according to their charge, a similar experiment was done with covesicles of pyPC/DMPM (70:30) mixed with excess unlabeled covesicles of POPC/DMPM (30:70) as acceptor. pyPC is a zwitterionic phospholipid, whereas pyPM is monoanionic, but both phospholipids were equally exchanged through MBP contacts between vesicles (data not shown). When pure pyPC vesicles were mixed with POPC/DMPM vesicles, no exchange of pyPC was induced by MBP, even in the presence of KCl, presumably due to poor binding of MBP to the PC vesicles. These results show that MBP binding is a necessary precondition for the formation of functional intervesicle contacts for the phospholipid exchange.

Exchange of Cationic Probe R18. The pyPM dequenching assay does not distinguish selective phospholipid exchange through intervesicle molecular contacts from lipid mixing due to fusion or hemifusion. The exchange through a contact should show selectivity as was shown by MBP-induced lipid mixing monitored as the release of self-quenching of R18 due to surface dilution of the probe with excess unlabeled vesicles. R18 (6 mol %) was incorporated in the outer membrane of preformed POPC/DMPM vesicles, and the labeled vesicles were then mixed with excess unlabeled POPC/DMPM vesicles. The relative change in fluorescence induced by MBP is shown in Figure 4A. At the lipid/MBP ratios where MBP induces significant vesicle aggregation (Figure 2), it does not induce any significant lipid mixing in the absence of salt. On the other hand, in the presence of 133 mM KCl, aggregation is accompanied by lipid mixing between the apposed vesicles (values corresponding to 15 min after KCl addition). It should be noted that KCl has no effect on the fluorescence of R18 under the same conditions

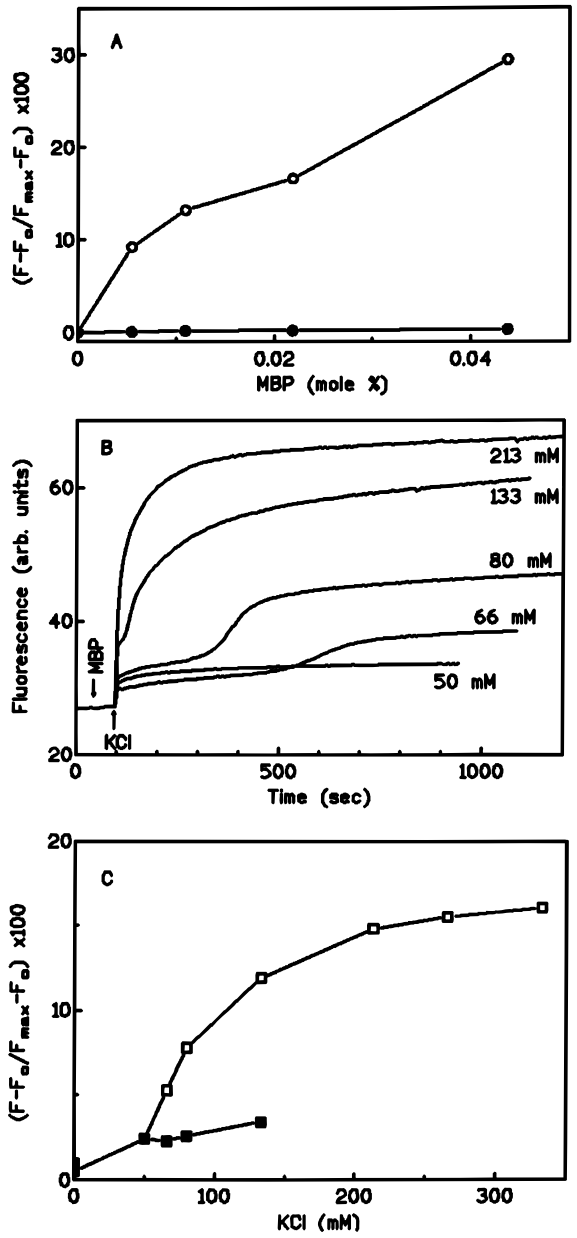

FIGURE 3: Changes in the pyrene monomer fluorescence emission intensity at 395 nm (excitation 346 nm) as a result of MBP-mediated transfer of pyPM from donor vesicles (1.7 μM pyPM/POPC) to acceptor vesicles (211 μM POPC/DMPM). (Panel A) Increase in fluorescence as a function of the mole fraction of MBP in the absence (●) and in the presence (○) of 133 mM KCl (15 min after salt addition). The order of addition was vesicles → MBP → KCl (as also in Figure 2). (Panel B) Time-course of the fluorescence change; MBP (0.047 μM) was added to the mixture of vesicles followed by KCl to the desired final concentration. (Panel C) Fluorescence values taken from panel B immediately after KCl addition at ≤133 mM KCl (■), and 15 min after addition of salt (□). In this and the following figures, MBP effect, if any, does not change with time for at least 1 h.

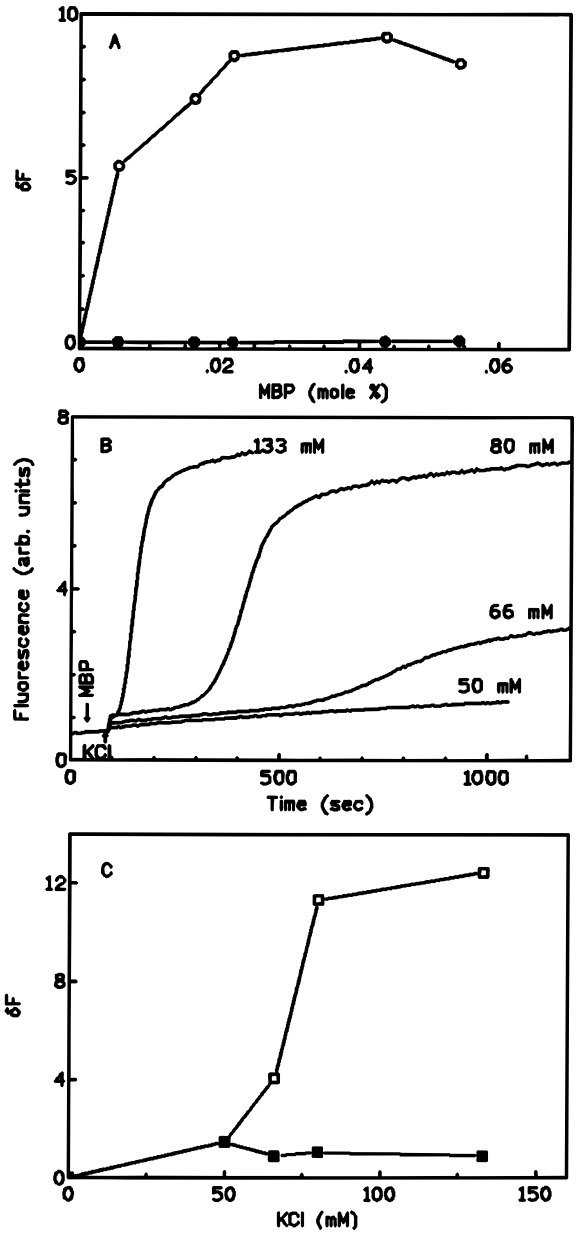

FIGURE 4: Increase in the emission due to dequenching of 6% R18 in POPC/DMPM vesicles (1.7 μM) mixed with POPC/DMPM vesicles (211 μM) induced by MBP. (Panel A) Increase in fluorescence as a function of MBP mole fraction in the absence (●) and in the presence (○) of 133 mM KCl (other details as in Figure 2); (Panel B) Time-course of fluorescence increase after addition of MBP (0.047 μM) to the mixture of labeled and unlabeled vesicles, followed by KCl at the indicated final concentrations. (Panel C) Fluorescence increase measured immediately after KCl addition (■), and 15 min after KCl addition (□). Excitation at 556 nm, emission at 577 nm.

as used in the assay with MBP. In conjunction with the results shown in Figure 3, it is clear that results with the two probes (pyPM and R18) are qualitatively similar, but quantitative differences are significant in the presence of KCl. As elaborated below, such quantitative differences at low salt concentrations suggest that the exchange of R18 is not favored under these conditions.

At this stage, the possibility of solubilization of vesicles by MBP is ruled out because this would cause a decrease in light scattering, not the observed increase (Figure 2). As was seen for the scattering change, the dilution of R18 follows a biphasic change at salt concentrations below 100 mM (Figure 4B), with an initial small but rapid increase in fluorescence after the addition of salt, followed by a lag phase and then an additional time-dependent increase. Nevertheless, the contribution of the second phase is much larger, whereas very little dilution of R18 occurs during the rapid phase, immediately after the addition of KCl (Figure 4B). The relative increase in fluorescence of R18 as a function of KCl added to vesicles containing 0.022 mol % MBP is shown in Figure 4C, where the contributions of the two phases are plotted. Here, the relative magnitudes of the two

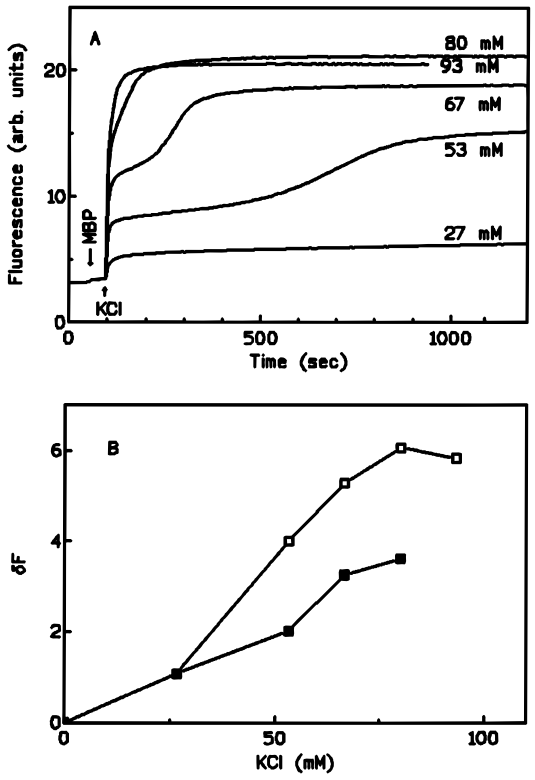

FIGURE 5: Increase in the emission due to dequenching of 20% Rh-PE in POPC/DMPM vesicles (1.7 μM) mixed with POPC/DMPM vesicles (211 μM) induced by MBP. (Panel A) Time-course of the increase of fluorescence after addition of MBP (0.047 μM) to the mixture of vesicles, followed by KCl to the indicated final concentrations. (Panel B) Fluorescence increase measured immediately after KCl addition to the MBP containing vesicles (■) or 15 min after KCl addition (□). Excitation 556 nm, emission 577 nm.

phases (the fast initial exchange and the second time-dependent one) are considerably different compared to that seen with pyPM (Figure 3, panels B and C) or pyPC (not shown), i.e., the first phase is greater relative to the second within the case of R18, whereas in pyPM and pyPC the two phases differ less. Such differences indicate sorting, or restriction for the exchange of cationic R18, in the first phase. This interpretation is consistent with the step 2 of Figure 1.

To determine if the sorting was due to a steric effect of rhodamine in the headgroup or to a charge effect because R18 is a cationic molecule, Rh-PE was included in the POPC/DMPM vesicles at a self-quenching concentration (20% was needed), and these vesicles were mixed with 125-fold excess unlabeled vesicles, followed by MBP (0.022 mol %) and KCl. As shown in Figure 5A, the two phases show a comparable change (Figure 5, panels A and B), as was the case with pyPM, but not with R18. Collectively, these results show that cationic R18 is initially excluded from the first phase of exchange through the vesicle−vesicle molecular contacts formed by cationic MBP in the presence of salt (corresponding to the step 2 of Figure 1) while Rh-PE is not. This sorting is probably by electrostatic repulsion, because zwitterionic Rh-PE and pyPC, or anionic pyPM, are not excluded in the step 2 (Figure 1).

The lag periods observed in the various protocols are virtually same, although the value does depend on the lipid composition. Typical reproducibility for the lag period is within less than 50 s, however in the Rh-PE exchange experiment (Figure 5) the value is significantly lower (Figures 2 and 4). This difference is primarily due to the difference in the phospholipid composition because when the 20% Rh-PE vesicles were used for the scattering runs the lag period was virtually the same as that seen in Figure 5. Similar experiments carried out under other conditions also showed that while the lag period depends on the lipid composition of vesicles, the overall behavior depends only on the presence of the anionic phospholipids but the structure of the phospholipid is not critical (also Figure 9).

Resonance Energy Transfer NBD-PE/Rh-PE to Monitor Vesicle Apposition and Lipid Exchange. Apposition of vesicles by MBP in the absence of KCl was also monitored by resonance energy transfer (RET) between POPC/DMPM vesicles containing donor NBD-PE probe to vesicles containing acceptor Rh-PE probe (0.6% each). RET distance for this pair is about 50 Å. As shown in Figure 6A, MBP causes an increase in RET, reflected as an increase of Rh emission intensity (592 nm) seen even at 0.01 mol % MBP, and the magnitude of the increase depends on the mole fraction of MBP. In the absence of KCl, the observed increase in RET is due to vesicle apposition, because the possibility of lipid-mixing under these conditions is discounted on the basis of results in Figures 3−5. To rule out the possibility of nonspecific lipid mixing at low MBP, we designed an experiment where covesicles containing both donor and acceptor probes (0.3% each NBD-PE and Rh-PE in a matrix of POPC/DMPM) were mixed with a 50-fold excess POPC/DMPM vesicles, and then titrated with increasing amounts of MBP. As shown in Figure 6A, there is no dilution of the probes even up to 0.1 mol % MBP, indicating that the observed increase in RET is due to vesicle apposition by MBP without lipid exchange. The possibility of fusion is further ruled out because such time-dependent changes are seen only at >0.6 mol % MBP (see also Figure 6C).

As expected, KCl increases the MBP-induced RET from NBD-PE containing vesicles to Rh-PE vesicles. Figure 6B shows the time course of the KCl induced fluorescence change at 592 nm (Rh-PE) by adding 80 mM or 133 mM KCl to a 1:1 mixture of POPC/DMPM vesicles (containing NBD-PE or Rh-PE) with 0.022 mol % MBP. The increase in RET induced by this small amount of MBP in the absence of KCl is only around 1% of the total, whereas a significant increase is seen with KCl (corresponding to 48% of the total at 80 mM KCl). Controls showed that KCl did not affect the RET in the absence of MBP, and MBP does not have any time-dependent effect on the RET emission. At 80 mM KCl, we see the fast increase in RET after addition of salt, followed by a lag period and then the second increase. The increase in RET between NBD and Rh vesicles induced by MBP in the presence of KCl is not only due to vesicle apposition, but also due to lipid mixing. This is because if MBP and KCl are added to a mixture of POPC/DMPM vesicles containing both probes (NBD and Rh) and unlabeled vesicles, it results in a decrease of RET, which is expected if lipid mixing and surface dilution of the probes take place (data not shown).

To determine the origin of the biphasic change seen in the fluorescence and light scattering as a function of time, at 0.022% MBP mole fraction and less than 100 mM KCl (Figures 2B−6B), we modified the RET experiment described above. By incubating the POPC/DMPM vesicles containing 0.6% NBD-PE with dithionite, prior to the addition of Rh-PE vesicles, the NBD-PE fluorescence of the

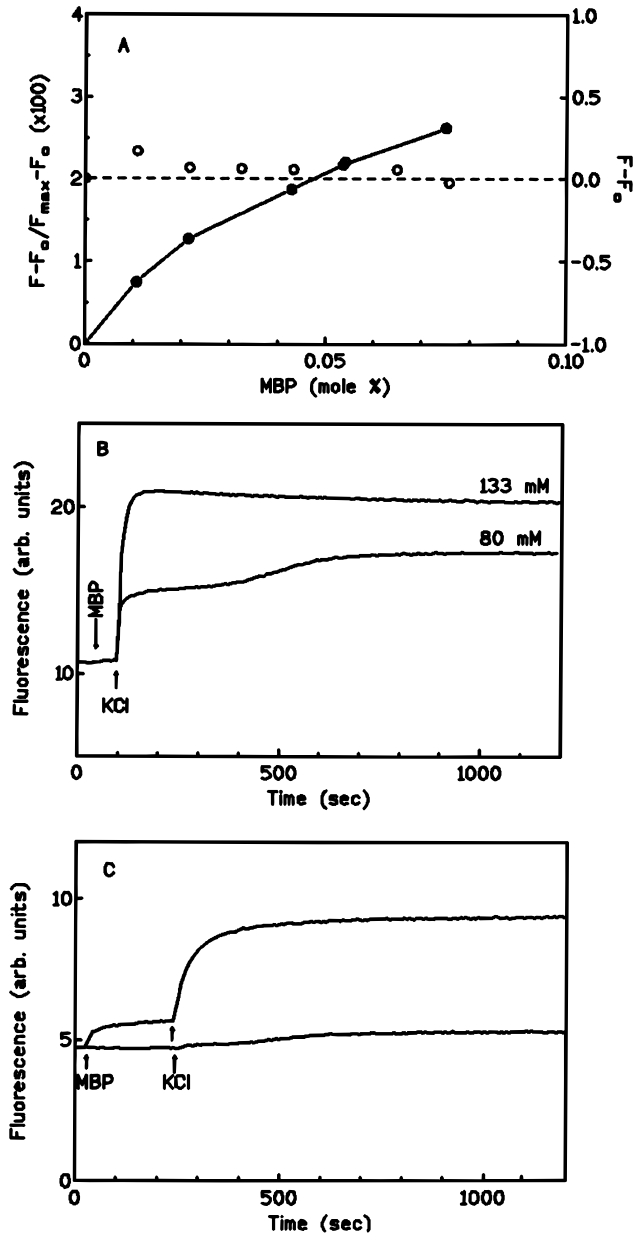

FIGURE 6: Resonance energy transfer from NBD-PE to Rh-PE to measure vesicle apposition and lipid mixing. (Panel A) Increase of fluorescence at 592 nm as a function of MBP added to a mixture of POPC/DMPM vesicles containing 0.6% NBD-PE (55 μM) and POPC/DMPM vesicles with 0.6% Rh-PE (55 μM), without KCl (●, left axis); and change in fluorescence ($F - F_o$) by addition of the same mole fraction of MBP to a mixture of unlabeled POPC/DMPM vesicles (1.0 mM) with vesicles of POPC/DMPM containing both NBD-PE and Rh-PE (0.3% each, lipid concentration 21.8 μM) (○, right axis). (Panel B) Time-course for the fluorescence change of a 1:1 mixture of vesicles with NBD-PE and vesicles with Rh-PE (110 μM total lipid) after addition of 0.022 mol % MBP and KCl. (Panel C) Same as in panel B but NBD-containing vesicles are labeled only in the inner monolayer; in the lower curve, MBP is 0.022 mol % and KCl is 80 mM; in the upper curve, MBP is 1.0 mol % and KCl is 133 mM.

outer leaflet was selectively lost. As will be described later, dithionite does not significantly permeate the membrane of POPC/DMPM vesicles over the time course of this experiment. In these asymmetrically labeled vesicles, only the NBD-PE groups that are in the inner leaflet of the vesicle are still fluorescent. Asymmetrically labeled vesicles were mixed with an equal amount (in moles) of Rh-PE-containing vesicles, and then MBP (0.022 mol %) and KCl were added

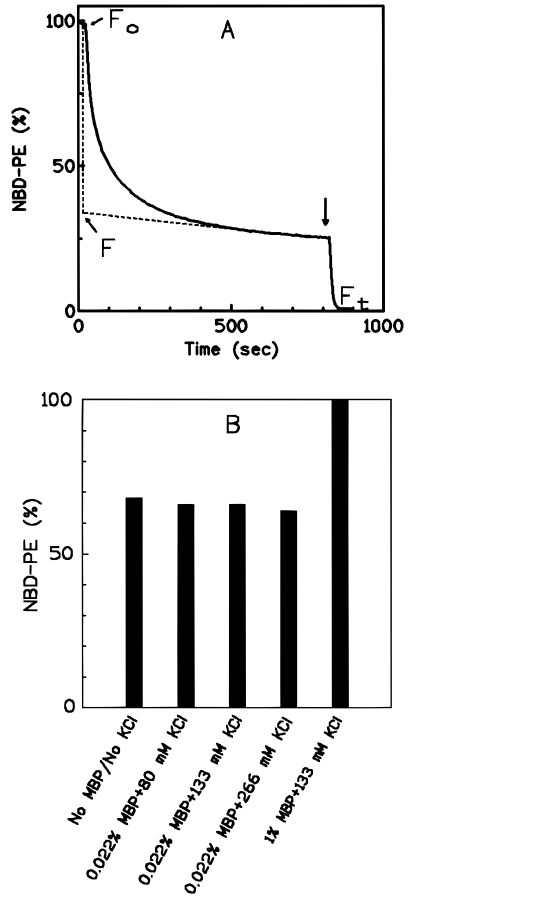

FIGURE 7: Reaction progress of POPC/DMPM vesicles containing 0.6 mol % NBD-PE (110 μM) with dithionite (20 mM). (Panel A) Amount of lipid reacted with dithionite as a function of time; at the end of the reaction, vesicles were disrupted with deoxycholate (2.2 mM, arrow) to allow reaction of the inner monolayer lipid. (Panel B) Total amount of phospholipid in the outer monolayer of vesicles calculated from plots like the one in Panel A calculated according to $[1 - (F - F_t)/(F_o - F_t)] \times 100$. Concentrations of MBP and KCl are indicated in the figure.

sequentially. As shown in Figure 6C (bottom), a very small increase in fluorescence is seen on the addition of 80 mM KCl, indicating that the RET seen for vesicles with label in both monolayers was due to phospholipid exchange between the outer leaflets of the vesicles apposed by MBP. A control experiment shown in Figure 6C (top) showed that, with high MBP mole fractions (1 mol %) and 133 mM KCl, there is an increase in RET intensity due to mixing of inner monolayers of the asymmetrically labeled vesicles.

Mixing of the Outer Monolayer Lipids of Apposed Vesicles Occurs Without Flip-Flop or Disruption of the Vesicles. Low concentrations of MBP do not disrupt POPC/DMPM vesicles, even in the presence of salt. This is demonstrated by the fact that addition of dithionite to sonicated dispersions of POPC/DMPM containing 0.6% NBD-PE, with or without MBP, results in a partial decrease in the fluorescence from NBD (Figure 7A). This is expected if only the probe in the outer monolayer of sonicated unilamellar vesicles is modified. The reaction starts immediately after the addition of dithionite, and it has two components: the fast phase is complete in less than 100 s, accompanied by a parallel slow decrease in fluorescence. We attribute the fast reaction to the reduction of the readily exposed lipid present in the outer monolayer of the vesicles. The slow rate of fluorescence decrease is possibly due to permeation of the membrane to

the reagent and reaction of the labeled lipid in the inner monolayer. Several controls support this hypothesis. For example, if the vesicles were disrupted with deoxycholate prior to addition of dithionite, all the labeled lipid reacted in less than 100 s, thus implying that the reaction with exposed NBD-PE lipid is very fast. Another possibility, that dithionite is exhausted in the cuvette over the time period of the reaction, was ruled out by adding a fresh aliquot of reagent at the end of the reaction. In this case, only a slight increase in the slower rate was observed, but not a rapid decrease in fluorescence as would be expected if there was more NBD-PE readily available for reaction.

The percentage of lipid present in the outer monolayer of the vesicles, was calculated as $[1 - (F - F_t)/(F_o - F_t)] \times 100$, where F is the fluorescence value obtained by extrapolating the slow reaction rate to time zero as shown in Figure 7A; F_t is the fluorescence after all the labeled lipid has reacted, calculated by adding deoxycholate; and F_o is the fluorescence of the vesicles prior to addition of dithionite. The fraction of dithionite quenched NBD does not change with the lipid/MBP ratio as well as salt concentrations, as summarized in Figure 7B. Under the conditions where there is aggregation of vesicles by MBP and outer layer lipid mixing by MBP and KCl, only 60 to 65% of the lipid remains exposed to the bulk aqueous compartment. These results show that vesicle leakage or solubilization does not occur and that flip-flop or transmonolayer movement of phospholipids is not promoted by bound MBP under any of these conditions. Other controls also showed that KCl does not interfere with the reaction of dithionite with POPC/DMPM/NBD-PE vesicles. As shown in Figure 7B, only at high concentrations of MBP (0.8 mol %) together with high salt concentration (133 mM) is all the lipid accessible to dithionite, indicating leakage and disruption of the bilayer barrier, as shown by direct experiments described next.

The Aqueous Contents of the Vesicles Do Not Leak or Mix During the Lipid Exchange. The leakage or mixing of aqueous contents induced by MBP with or without KCl was monitored by the ANTS/DPX fusion assay (Ellens et al., 1985) with some modifications. To determine the ability of our system to detect fusion, vesicles containing both ANTS and DPX were incubated with $CaCl_2$, which showed a time-dependent dequenching of ANTS fluorescence, indicative of leakage during Ca^{2+}-induced fusion (not shown). This control showed that we could use this assay to determine MBP-induced leakage of aqueous contents. As shown in Figure 8, MBP at 0.022 mol % does not cause leakage, even after addition of KCl at the concentrations where there is lipid exchange. Leakage was observed only at high MBP concentrations and 133 mM KCl. As indicated earlier, this is expected on the basis of results in Figure 7B.

The possibility that MBP induces non-leaky fusion was tested by mixing the two populations of vesicles, one with encapsulated ANTS and the other with DPX. Addition of MBP (0.022 mol %) and KCl, which does not induce leakage as shown in Figure 8, did not reveal any significant level of MBP-dependent nonleaky fusion. Ca^{2+}-induced fusion under the same conditions appears to be leaky, although we did not investigate it in detail. This behavior is expected in terms of the sequence of events shown in Figure 1, steps 2 and 3.

Specificity for Anionic Phospholipids. MBP does not bind to zwitterionic interfaces, however binding to anionic (co)-vesicles is seen irrespective of the nature of the lipid.

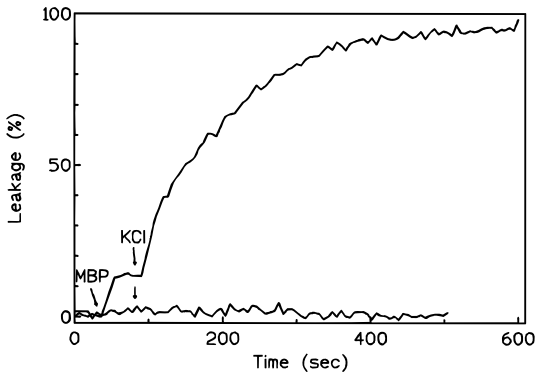

FIGURE 8: Release of ANTS/DPX coencapsulated in POPC/DMPM vesicles (217 μM) by (bottom) 0.022 mol % MBP and 133 mM KCl and (top) 0.22 mol % MBP and 133 mM KCl. Excitation was set at 360 nm, emission at 530 nm.

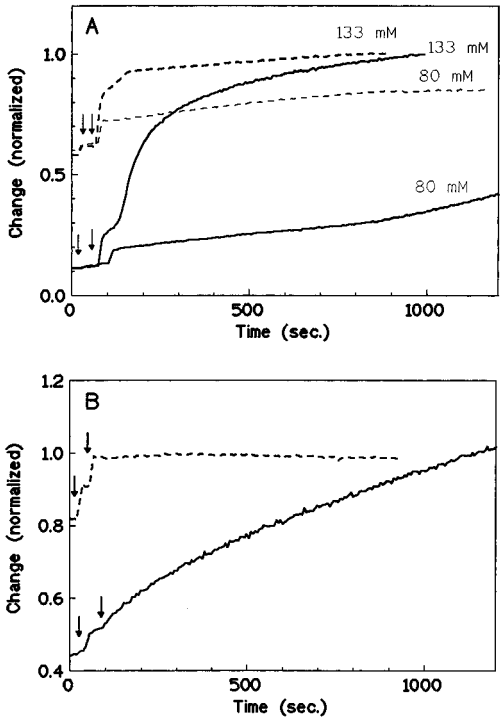

FIGURE 9: (A) Time-course of the change in the (dashed) scattering or (continuous) fluorescence due to surface dilution of R18 on the addition of 0.022 mol % MBP (at the first arrow) followed by indicated final concentration of KCl (at the second arrow) to covesicles of 211 μM DMPG/POPC (7:3 mole ratio). (B) Time-course of the change in the (dashed) scattering or (continuous) R18 fluorescence due to surface dilution on the addition of 0.022 mol % MBP (at the first arrow) followed by 133 mM KCl (at the second arrow) to covesicles of 211 μM POPG/POPC (2:8 mole ratio). Other conditions as in Figure 2 or Figure 4.

Quantitative differences seen with the lipid composition are often difficult to resolve because the competing processes are difficult to deconvolute at low lipid/MBP ratios. Therefore, it was of interest to see whether the MBP-induced exchange depends on the nature of the phospholipid head group. Spot checks indicated that DMPM can be replaced by other anionic lipids without any qualitative difference in the behavior. For example, as shown in Figure 9A, the salt effect on time-course of the change in the scattering of DMPG/POPC (3:7) covesicles is comparable to that of DMPM/POPC vesicles (Figure 2). As also shown in Figure 9A, dilution of R18 (as in Figure 4) tracks the change in the scattering but with a noticeable lag because the hemifusion

follows the aggregation step (Figure 1). Such a lag is more pronounced at lower mole ratios of anionic lipids in covesicles. Results in Figure 9B show that the scattering change is rapid and the dilution of R18 is considerably slower for POPG/POPC (2:8) covesicles at 133 mM KCl. These results clearly show that the R18 dilution is time-resolved from the scattering change. Also it is quite likely that the steady state number of aggregates in the presence of salt may remain small, yet the overall exchange of the probe will be large if MBP exchanges between vesicles to form new contacts (see below). Thus, even at lipid/MBP ratio of 4500, both the scattering and R18 dilution (hemifusion) occurs irrespective of the nature of the head group, chains, or charge density. The basis for the differences in the time-course was not investigated; however, such differences can be attributed to differences in the kinetics of not only the steps shown in Figure 1, but also the competing processes such as fusion, bilayer collapse, and leakage which predominate at lower lipid/MBP ratios used for most of the studies reported in the literature.

Binding of MBP to POPC/DMPM Vesicles Is Not Affected by KCl. As shown in Figure 2C, the maximum change in scattering induced by MBP in the presence of >100 mM KCl shows a decrease at ~1000 s. As an explanation, we considered the possibility that salt promotes desorption or redistribution of bound MBP in contacts. This would reduce the scattering without any effect on the maximum signal in the lipid mixing assays (e.g., Figure 3B). The possibility of desorption of MBP from the interface is ruled out by results shown in Figure 10. The stoichiometry for high affinity binding of MBP to the vesicles of POPC/DMPM containing 2% of either NBD-PE or DTPE-DNS was determined by the increase of intensity of the RET at 535 nm from the tryptophan residue of MBP to the acceptor at the interface. As shown in Figure 10A, essentially the same binding isotherms were obtained using both probes, with a plateau above a molar ratio of protein to lipid of 1:36. A ratio of 1:25 is obtained if we consider only the anionic DMPM. The same stoichiometry of binding was obtained in the presence of 106 mM KCl (Figure 10A). As also shown in Figure 10B for vesicles of POPC/DMPM/DHPE-DNS, with 0.021 MBP mole fraction, virtually the same intensity of RET was obtained at different concentrations of KCl. These results show that KCl does not promote desorption of bound protein, because this would result in a decrease of RET intensity from Trp to the Dansyl group in the vesicles. Note that there is a no time-dependence of the RET signal from the binding of MBP to vesicles or on the addition of salt, and the same signal intensity was obtained on sequential addition of MBP or by single addition of a larger aliquot.

Bound MBP Does Not Exchange in the Absence of KCl. A possibility to account for the KCl-dependent increase in aggregation of vesicles and lipid mixing induced by MBP, is that salt induces exchange of MBP between vesicles. Results in Figure 11A show that MBP bound to POPC/DMPM vesicles does not exchange in the absence of salt. Binding of MBP to vesicles of POPC/DMPM containing 2% NBD-PE (0.05 mol % MBP) results in significant RET from the tryptophan of MBP to the NBD groups at the interface (Figure 11A, spectrum *a*). The RET intensity at ~530 nm does not change by subsequent addition of the same amount of unlabeled vesicles (not shown, but superimposable to spectrum a). On the other hand, if MBP is added to the

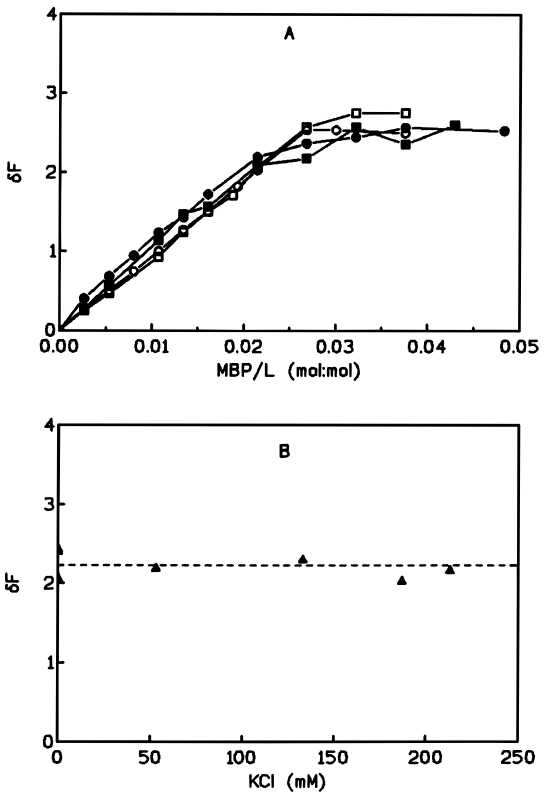

FIGURE 10: (Panel A) Binding of MBP to POPC/DMPM vesicles (21.76 μM) containing 2% of NBD-PE (circles) or 2% DHPE-DNS (squares): RET intensity from Trp of MBP to the label at the interface was measured at 535 nm (excitation at 285 nm). (○) and (□) titration in 10 mM Tris/1 mM EGTA; (●) and (■) titration in 10 mM Tris/1 mM EGTA/106 mM KCl. (Panel B) RET intensity at 535 nm as a function of KCl concentration. POPC/DMPM vesicles with 2% DHPE-DNS containing 0.021 mole fraction of MBP were titrated with KCl from a stock solution (4 M).

unlabeled POPC/DMPM vesicles prior to the addition of labeled vesicles (spectrum c), no significant RET is seen, confirming that bound MBP does not exchange with vesicles added afterward and also indicating that the labeled lipid does not exchange. If MBP (0.027 mol %) is added to the mixture of labeled and unlabeled vesicles (spectrum b), an intermediate level of RET intensity is obtained, as expected from a homogeneous distribution of MBP between labeled and unlabeled vesicles. Together these results show that in the absence of KCl, MBP remains bound and does not exchange between vesicles.

When the experiments described above were carried out in the presence of 133 mM KCl, all the three orders of addition yielded the same spectra (Figure 11B), indicating that MBP, or the lipid, or both, exchange readily between the vesicles in contact. The same results were obtained from the protocol of exchange of pyPM between vesicles induced by MBP (as shown in Figure 3). High mole fraction of MBP (for example 0.22 mol %), even in the absence of KCl, promotes a noticeable (≈1%) exchange of pyPM from POPC/pyPM vesicles to excess POPC/DMPM vesicles. If POPC/DMPM vesicles are premixed with MBP and then labeled POPC/pyPM vesicles are added, no significant increase in pyrene monomer fluorescence (395 nm) is seen, indicating that there is no lipid mixing with the vesicles added afterward, i.e., MBP added to POPC/DMPM vesicles remains bound and does not exchange. An increase in monomer fluorescence results if at this point KCl is added.

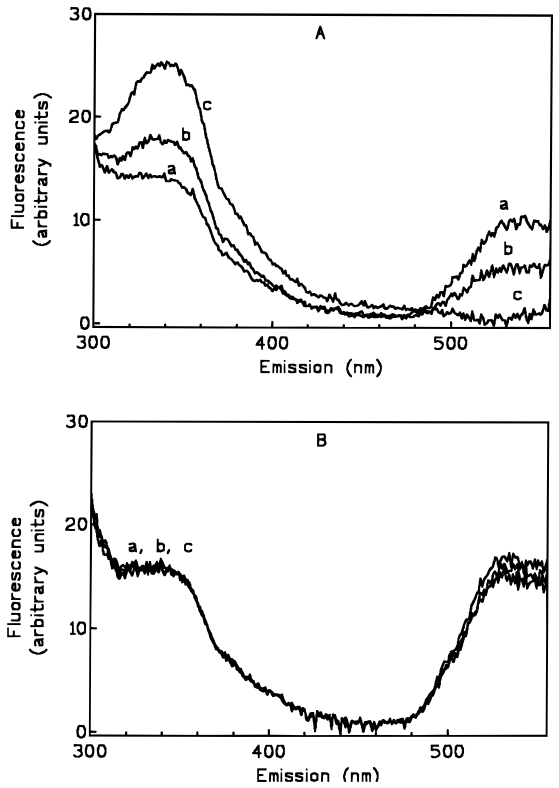

FIGURE 11: RET from Trp of MBP to POPC/DMPM vesicles containing 2 mol % NBD-PE. (Panel A) Spectrum a: MBP (0.58 μM) was added to labeled vesicles (1.08 mM), and then POPC/DMPM unlabeled covesicles (1.06 mM) were added. Spectrum b: MBP was added to a mixture of labeled and unlabeled vesicles. Spectrum c: MBP added to unlabeled vesicles, followed by labeled vesicles. (Panel B) Same as in panel A but 133 mM KCl was added in every case to the vesicles and MBP mixture. Excitation was 285 nm.

DISCUSSION

In this paper we have shown that MBP in the presence of salt (KCl) induces hemifusion, but not fusion, of anionic vesicles of POPC/DMPM. In fact, by adopting the spectroscopic methods, we could distinguish three sequential steps that lead to hemifusion of vesicles. In the absence of salt, aggregation of vesicles is induced by MBP without fusion or exchange of lipids between apposed vesicles (step 1, Figure 1). Addition of KCl to a population of anionic vesicles containing 0.022 mol % MBP results in lipid mixing between the outer monolayers of the vesicles in contact. This satisfies the criterion for hemifusion, i.e., the contacting leaflets of apposed vesicles become continuous. This process occurs in two phases, represented as steps 2 and 3 in Figure 1. *First*, a fast mixing of lipids with some specificity for the molecules that can be exchanged; for example, cationic R18 is excluded, whereas anionic and zwitterionic phospholipids, such as pyPC, pyPM, and Rh-PE are exchanged. *Second*, after a lag phase, larger aggregates are formed and nonspecific mixing of phospholipids and probes in the outer monolayers occurs without mixing of inner monolayers or leakage of aqueous contents. These steps are clearly distinguishable with a judicious combination of ionic strength and lipid/MBP ratio. Although we have carried out detailed studies with DMPM as the anionic lipid, note that the behavior with POPG, DMPG, and the various labeled lipids is similar. Kinetic differences are expected because the key variables (charge density, MBP/lipid ratio) control not only the steps explicitly considered in Figure 1, but also the propensity toward the competing processes such as leakage, fusion, and collapse of vesicles. At the MBP concentrations used in the present study, the competing processes are ruled out. Broader implications of the MBP-induced lipid exchange triggered by KCl are discussed below.

Molecular Contacts between Vesicles. Direct and selective intervesicle exchange of phospholipids through protein-mediated contacts is a novel yet complex phenomenon (Cajal et al., 1996a,b). By spectroscopic protocols, combined with methods based on the scooting kinetics by phospholipase A2 on anionic vesicles (Jain et al., 1995), we have shown that the polycationic peptide polymyxin B (PxB) forms molecular contacts between anionic vesicles (Cajal et al., 1995, 1996a). It is remarkable that PxB-contacts allow a selective and rapid exchange of phospholipids (Cajal et al., 1996b). Vesicle−vesicle PxB-contacts share some features with the MBP-contacts described in this paper. In both cases, stable contacts are formed with a very small number of peptide or protein molecules per vesicle; only the phospholipids from the outer monolayers of the vesicles in contact exchange, whereas the inner monolayers (distal) remain intact; the aqueous contents of the vesicles do not mix or leak. However, there are some important differences. PxB-contacts are not perturbed by salt, whereas MBP-contacts permit exchange of phospholipids only in the presence of salt. In addition, the onset of the exchange of phospholipids through PxB-contacts is very fast ($<$10 s) and is selective only for monoanionic phospholipids, whereas MBP-mediated contacts exhibit complex kinetics with modest selectivity for the exchange or sorting of molecules only in the initial rapid phase. Nonselective time-dependent mixing seen at the end of the lag phase suggests that hemifusion has occurred. It is possible that the two phases are associated with two different conformational or aggregated forms of MBP. Both of these processes, which we are trying to characterize, may be related.

Physiological Role of MBP-Contacts. Several critical physiological functions in the cell involve the establishment of contacts between two membranes. For example, membrane contacts are a necessary first step for vesicle formation and fusion, as implicated in budding, targeting, endo- and exocytosis, fertilization, cell division and vesicular transport of newly synthesized lipids and proteins to their final destinations within the cell (White, 1992; Moreau & Cassagne, 1994; Rothman, 1996). In all such processes, certain constraints must control the fluxes of components present or associated with the membranes, so that the compositional identity of membranes in contact is not compromised. Although many details remain to be established, the generally accepted view is that all the processes of vesicular transport could utilize the same or very similar molecular machinery and that specific proteins facilitate merger of lipid membranes, target selection, and regulation of fusion (Hoekstra, 1990; Ferro-Novick & Jahn, 1994; Hughson, 1995; Schweizer et al., 1995; Südhof, 1995; Rothman, 1996). Molecular contacts mediated by PxB and MBP are useful experimental models for understanding the mechanisms of membrane interactions and lipid dynamics. Protein or peptide-mediated membrane−membrane molecular contacts capable of selective exchange between bilayers without fusion offer a conceptual prototype to explore mechanisms involved in trafficking and sorting of phospholipids between

cellular compartments. For example, the salt-triggered hemifused state stabilized by MBP is conceptually similar to the one induced by GPI-anchored influenza hemagglutinin (GPI-HA) between red blood cells and GPI-HA-expressing cells (Kemble et al., 1994; Melikyan et al., 1995). The trigger in the case of GPI-HA is a decrease in pH. In both cases the trigger is followed by selective mixing of the monolayers in contact without merger of distal monolayers or mixing of aqueous compartments. Thus, contacts and hemifused state induced by MBP provide a prototype worthy of detailed investigation.

REFERENCES

Ballanyi, K., & Kettermann, H. (1990) *J. Neurosci. Res. 26*, 455−460.

Boggs, J. M., Moscarello, M. A., & Papahadjopoulos, D. (1977) *Biochemistry 16*, 5420−5426.

Boggs, J. M., Stollery, J. G., & Moscarello, M. A. (1980) *Biochemistry 19*, 1226−1234.

Boggs, J. M., Wood, D. D., & Moscarello, M. A. (1981) *Biochemistry 20*, 1065−1073.

Boggs, J. M., Moscarello, M. A., & Papahadjopoulos, D. (1982) in *Lipid-Protein Interactions* (Jost, P., & Griffith, O. H., Eds.) Vol. 2, Chapter 1, pp 2−43, John Wiley & Sons, Inc., New York.

Brunner, C., Lassmann, H., Waehneldt, T. V., Matthieu, J. M., & Linington, C. (1989) *J. Neurochem. 52*, 296−304.

Cajal, Y., Berg, O. G., & Jain, M. K. (1995) *Biochem. Biophys. Res. Commun. 210*, 746−752

Cajal, Y., Rogers, J., Berg, O. G., & Jain, M. K. (1996a) *Biochemistry 35*, 299−308.

Cajal, Y., Ghanta, J., Easwaran, K., Surolia, A., & Jain, M. K. (1996b) *Biochemistry 35*, 5684−5695.

Cheifetz, S., & Moscarello, M. A. (1985) *Biochemistry 24*, 1909−1914.

Cheifetz, S., Moscarello, M. A., & Deber, C. M. (1984) *Arch. Biochem. Biophys. 233*, 151−160.

Chiu, S. Y. (1991) *Glia 4*, 541−558.

Chou, F. C. H., Chou, C. H. J., Shapira, R., & Kibler, R. F. (1976) *J. Biol. Chem. 251*, 2671−2676.

Düzgüneş, N., & Wilschut, J. (1993) *Methods Enzymol. 220*, 3−14.

Ellens, H., Bentz, J., & Szoka, F. C. (1985) *Biochemistry 24*, 3099−3106.

Epand, R. M., Dell, K., Surewicz, W. K., & Moscarello, M. A. (1984) *J. Neurochem. 43*, 1550−1555.

Ferro-Novick, S., & Jahn, R. (1994) *Nature 370*, 191−193.

Gould, R. M., & London, Y. (1972) *Biochim. Biophys. Acta 290*, 200−218.

Hoekstra, D. (1990) *J. Bioenerg. Biomembr. 22*, 121.

Hoekstra, D., & Düzgüneş, N. (1993) *Methods Enzymol. 220*, 15−31.

Hoekstra, D., Buist-Arkema, R., Klappe, K., & Reutelingsperger, C. P. M. (1993) *Biochemistry 32*, 14194−14202.

Hughson, F. M. (1995) *Curr. Opin. Struct. Biol. 5*, 507−513.

Jain, M. K., & Vaz, W. L. C. (1987) *Biochim. Biophys. Acta 905*, 1−8.

Jain, M. K., Rogers, J., Jahagirdar, D. V., Marecek, J. F., & Ramirez, F. (1986) *Biochim. Biophys. Acta 860*, 435−447.

Jain, M. K., Rogers, J., Berg, O., & Gelb, M. H. (1991) *Biochemistry 30*, 7340−7348.

Jain, M. K., Gelb, M. H., Rogers, J., & Berg, O. G. (1995) *Methods Enzymol. 249*, 567−614.

Jo, E., & Boggs, J. M. (1995) *Biochemistry 34*, 13705−13716

Jones, A. J. S., & Epand, R. M. (1980) *Biochim. Biophys. Acta 625*, 165−178.

Kemble, G. W., Danieli, T., & White, J. M. (1994) *Cell 76*, 383−391.

Kettenman, H., (1987) *Can. J. Physiol. Pharmacol. 65*, 1033−1037.

Lampe, P. D., Wei, G. J., & Nelsestuen, G. L. (1983) *Biochemistry 22*, 1594−1599.

McIntyre, J. C., & Sleight, R. G. (1991) *Biochemistry 30*, 11819−11827.

Melikyan, G. B., White, J. M., & Cohen, F. S. (1995) *J. Cell Biol. 131*, 679−691.

Moreau, P., & Cassagne, C. (1994) *Biochim. Biophys. Acta 1197*, 257−290.

Omlin, F. X., Webster, deF., Palkovits, C. G., & Cohen, S. R. (1982) *J. Cell. Biol. 95*, 242−248.

Papahadjopoulos, D., Cowden, M., & Kimelberg, H. (1973) *Biochim. Biophys. Acta 330*, 8−26.

Papahadjopoulos, D., Moscarello, M. A., Eylar, E. H., & Isac, T. (1975) *Biochim. Biophys. Acta 401*, 317.

Rothman, J. E. (1996) *Protein Sci. 5*, 185−194.

Schweizer, F. E., Betz, H., & Augustine, G. J. (1995) *Neuron 14*, 689−696.

Smith, R. (1977) *Biochim. Biophys. Acta 470*, 170−184.

Smith, R., & McDonald, B. J. (1979) *Biochim. Biophys. Acta*, 133−147.

Südhof, T. (1995) *Nature 375*, 645−653.

Walker, A. G., & Rumby, M. G. (1985) *Neurochem. Int. 7*, 441−447.

White, J. M. (1992) *Science 258*, 917−924.

BI962232+